

**KERNFORSCHUNGSZENTRUM
KARLSRUHE**

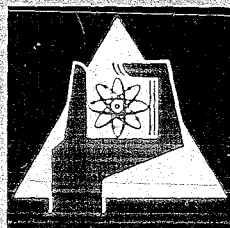
July 1970

KFK 1190

Institut für Angewandte Kernphysik

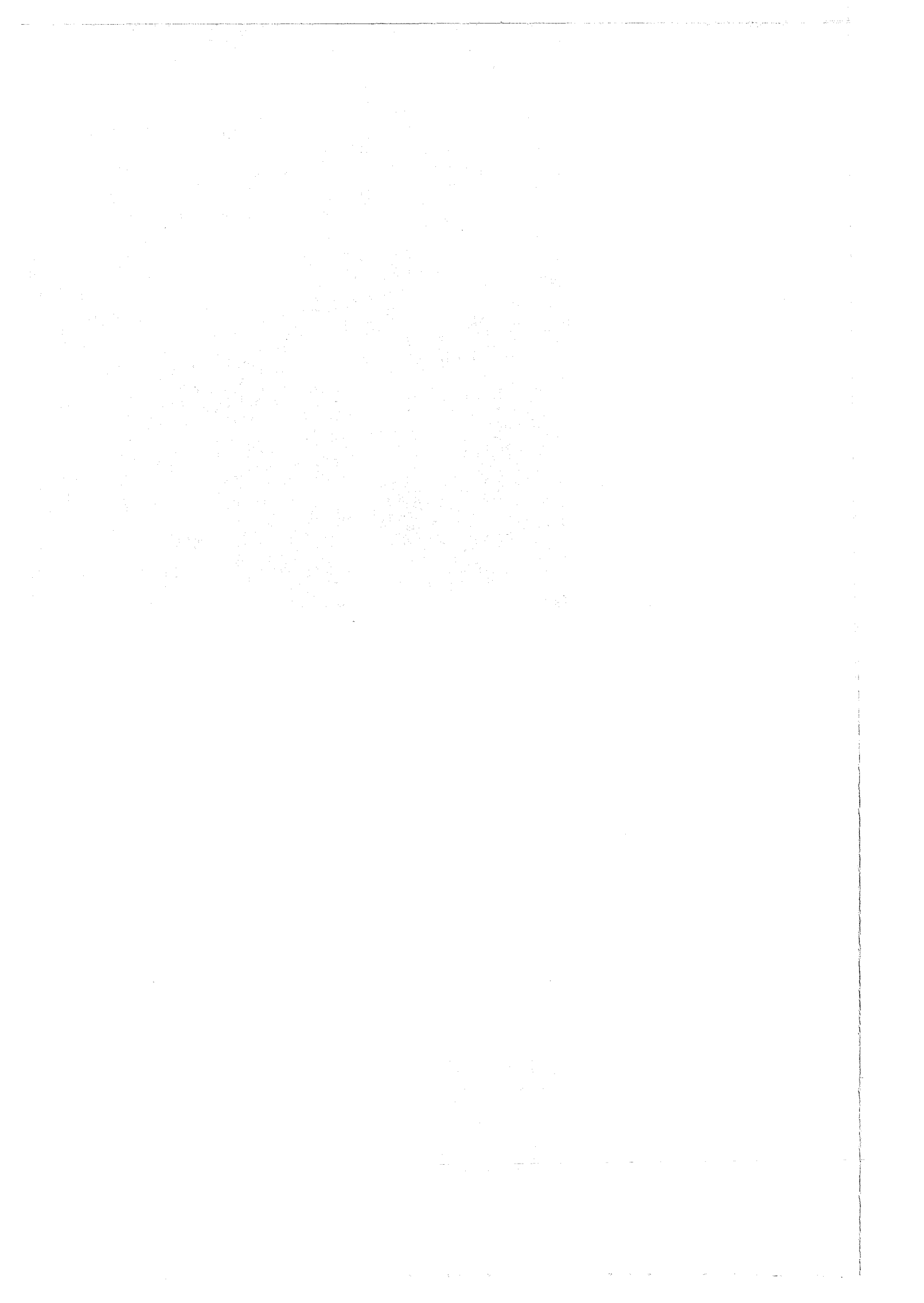
Excitation Functions and Differential Cross Sections for the
 $\text{Be}^9(n, \alpha)$ Reaction with 8 to 30 MeV Neutrons

L. Kropp, P. Forti



GESELLSCHAFT FÜR KERNFORSCHUNG M. B. H.

KARLSRUHE



KERNFORSCHUNGSZENTRUM KARLSRUHE

July 1970

KFK 1190

Institut für Angewandte Kernphysik

Excitation Functions and Differential Cross Sections for the
 $\text{Be}^9(n,\alpha)$ Reaction with 8 to 30 MeV Neutrons

by

L. Kropp and P. Forti*

Gesellschaft für Kernforschung m.b.H., Karlsruhe

* Now at LABEN Lab., Milan, Italy

Abstract

A new four parameter time-of-flight experiment (particle type and energy, neutron energy and emission angle) yielding differential cross section data of neutron-induced reactions was performed. Energy distributions of α -particles from the ${}^9\text{Be}(n,\alpha)$ reaction were measured at several angles for neutron energies ranging from 8 to 30 MeV. Angular distributions and excitation functions for the three lowest states of He^6 (ground state, 1.7 and 3.4 MeV) are evaluated.

Zusammenfassung

Es wurde ein neues Vier-Parameter-Flugzeitexperiment (Teilchenenergie und -art, Neutronenenergie und Reaktionswinkel) zur Bestimmung differentieller Wirkungsquerschnitte Neutronen-induzierter Reaktionen durchgeführt. Für Neutronenenergien zwischen 8 und 30 MeV wurden unter verschiedenen Winkeln die Energieverteilungen emittierter α -Teilchen der ${}^9\text{Be}(n,\alpha)$ Reaktion gemessen. Die Winkelverteilungen und Anregungsfunktionen für die Übergänge zum Grundzustand und den ersten angeregten Zuständen bei 1.7 und 3.4 MeV im He^6 -Kern wurden bestimmt.

1. Introduction

In this report differential cross section data for the ${}^9\text{Be}(n,\alpha)$ reaction in the energy region from 8 to 30 MeV are presented*. The neutron induced reactions were measured in a four parameter time-of-flight experiment using the Karlsruhe isochronous cyclotron as an intense neutron source. The novel method applied was to determine during one single run all four parameters - neutron energy, particle energy, particle type and reaction angle.

This paper is intended to give a summary of the evaluated experimental data for the ${}^9\text{Be}(n,\alpha)$ reaction and a comparison with data available. A detailed description of the experimental arrangement is in preparation.

2. Experimental Lay-out

The principle of the measurement was to record at different reaction angles the particles emitted from nuclei bombarded by neutrons with a continuous energy spectrum incident on a thin target foil, to separate the distinct kinds of particles, and to measure their energy.

The cyclotron was used to produce the neutrons via the (d,n) reaction on thick Be or C blocks. The normal recurrence frequency of the deuteron pulses in the cyclotron was reduced by a factor of three to avoid overlap problems in the neutron time-of-flight measurement. Two out of the three ion bunches that are accelerated in normal continuous cyclotron operation were suppressed by axial beam deflection¹⁾. Thus, every 90 ns deuterons hit the cyclotron beam stop and produced bursts of neutrons with a continuous energy spectrum. The phase width of the internal deuteron beam²⁾ limits the length of the initial neutron burst to about 1 ns.

* An early phase of this work was reported at the Frühjahrstagung der Deutschen Physikalischen Gesellschaft (Freudenstadt, March 1969)

With the target located at a distance of 4.22 m from the neutron source, time-of-flight measurements were possible without overlap of neutrons from the preceding bursts. At this distance a neutron flux of at least $3 \cdot 10^7$ n/MeV cm²sec in the spectrum between 10 and 30 MeV was obtained.

A set of four counter telescopes each consisting of two silicon semiconductor detectors (60 and 500 thick) were located about 11 cm from the 4.75 mg/cm² thick Be-target. The telescopes positioned at different angles fulfilled a fourfold purpose: (i) they measured the particle energy; (ii) the type of particle was determined from the specific energy loss in the thin transmission detector and the total energy measured; (iii) the neutron time-of-flight was derived from a fast output pulse of the detectors; and (iv) the angular position yielded the information at different angles. By interchanging the telescopes a verification of the identity of information from the different telescopes was possible.

A problem was encountered in using the semiconductors for time-of-flight measurements. Usually, the output pulses from semiconductors are slow because of charge amplification. Using a technique proposed by Papadopoulos³⁾, fast output pulses were obtained. Over a wide dynamic range of charged particle energy good time information could be derived. Calculating the time-of-flight of the charged particle, the time of reaction and thus the time-of-flight of the neutron was determined. From this an overall energy resolution of 640 and 1800keV at neutron energies of 10 and 20 MeV was obtained.

Because of the large number of parameter combinations the data were transferred event by event via a CDC 3100 to magnetic tape. Data reduction such as particle identification and time-of-flight calculation was performed in part on-line; data accumulation and cross section evaluation were done off-line with an IBM 7074 computer.

The measurements were corrected for background events by a separate measurement without target. As the particle energies measured are lowered by the energy loss the particles suffered in the target, the energy values were corrected by an amount equal to the energy loss in half the sample thickness.

The absolute cross section values were determined by normalizing to the proton yield measured with a telescope of three detectors using the known n-p differential cross section data⁴⁾. The error in the absolute scale is about 7 - 10 % mainly due to counting statistics and the accuracy of the differential n-p cross section.

3. Experimental Results and Discussion

As an example of the energy distribution of α -particles emitted by the interaction of neutrons, the dependence of the cross section on angle for $E_n = 21.2$ MeV is shown in fig. 1. The arrows indicate the expected position of peaks for the transitions to the lowest states in ${}^6\text{He}$ ⁵⁾. From the decay of the excited states of ${}^6\text{He}$ and the many particle decay modes of (${}^9\text{Be}+n$), like $2n + 2\alpha$ or $2n + {}^8\text{Be}$ then decaying into two α 's, a continuous energy spectrum is built up below the two body decay α -peaks. Typical statistical errors are given in the 20° measurement. Peaks are not well separated as the particle energy resolution is strongly influenced by their energy loss in the target at lower particle energies (indicated as horizontal bars at the top of fig. 1) and by the moderate neutron energy resolution at higher neutron energies. The error bars in the 40° measurement contain the uncertainties due to target thickness effects ($\Delta E_\alpha(\rho\Delta x)$) and time resolution ($\Delta E_\alpha(\Delta E_n)$). The α -particle spectra are distorted at some energies by the presence of residual nuclei like ${}^6\text{He}$ or ${}^7\text{Li}$. They cannot be separated below the energy of α -particles which have a range in Si equal to the thickness of the transmission counter. Their expected energy values are assigned in the spectra.

Double differential cross section data for the emission of α -particles measured for reaction angles of 20 to 100° in the lab. system are given in figs. 2a-e. The evaluated data span an energy range for incident neutrons from 8 - 30 MeV. Cross sections in mb/sr MeV are plotted versus α -particle energy. The arrows not assigned indicate the expected α -peak position for the transitions to the levels in ${}^6\text{He}$. At higher neutron energies other reaction channels are open yielding more Li- or He-nuclei. They are denoted by arrows in the figures. The error bars below the parameter of neutron energy represent the uncertainty of α -particle energy due to time resolution. It is constant within 5 % over the whole particle energy range for one angle and neutron energy.

The angular distribution of emitted α -particles with energies corresponding to the excitation of the three lowest states in ${}^6\text{He}$ are shown for neutron energies above 11 MeV in fig. 3. The cross section values were extracted from the α -energy spectra or the spectra of the ${}^6\text{He}$ -recoil nuclei. As the α -peaks are not separated because of the moderate energy resolution, the integration of each α -group was performed as follows: given the position and the width expected the peaks were analysed mathematically by least squares fitting with gaussian distributions. The error bars for these differential cross sections given in the figure were determined from shifting the α -peak position left and right by about 220 keV and integrating these shifted peaks. The horizontal error bars represent the angular aperture of the target detector assembly.

The (n, α_0) cross section data are free from contributions of many particle decay modes because of kinematical considerations while the (n, α_1) and (n, α_2) data are not. The lines through the data points are drawn to give a continuous shape to the cross section over the plane spanned by neutron energy and reaction angle.

The marked angular dependence in all distributions is suggestive of a direct reaction mechanism as one should expect for such a light particle. So-called heavy particle reactions are indicated by the prominent backward peaking. The peaking near 70° to 80° c.m. angle and the forward rise in the distributions, respectively, can be interpreted as due to pick-up or knock-out processes.

A comparison of the shape of the angular distributions for the (n,α) transitions with cut-off plane-wave calculations (knock-out or pick-up plus one heavy-particle process)⁶⁾ yields good agreement with appropriate values for the cut-off radii⁷⁾. From the α -particle model of ${}^9\text{Be}$ ⁸⁾ the knock-out process may be favored. The pick-up process may be excluded because of the very improbable (${}^3\text{He} + {}^6\text{He}$)-cluster structure of ${}^9\text{Be}$.

The comparison of the measured angular distribution at 14.4 MeV neutron energy with data available⁹⁾ is shown in fig. 4. Because of the lack of extensive differential data further comparisons are not possible. The line drawn in fig. 4 reflects the shape in fig. 3. Both distributions show good agreement except for the value at 25° and the line drawn seems to underestimate the cross section near 65° given in ref. 9.

The excitation functions for the transitions to the three lowest states of ${}^6\text{He}$ measured at different angles are presented in figs. 5a-c. The errors shown are the same as in fig. 3. The neutron energy resolution is 640 keV at 10 MeV, 1.8 MeV at 20 MeV, and 3.3 MeV at 30 MeV. At the upper energy scale known ${}^{10}\text{Be}$ compound states⁵⁾ are indicated by arrows. Fig. 5 shows that the excitation functions are more or less monotonically decreasing functions of energy. An exception is seen in the presentation at $\theta_L = 40^\circ$ for the (n,α_0) transition where a dip is to be seen in the cross section at 10.5 MeV but cannot be observed at any other angle or excitation state of ${}^6\text{He}$. Near 18 MeV incident energy a broader maximum is indicated in some cases: at $\theta_L = 80^\circ$ for (n,α_0) , at $\theta_L = 20^\circ$ for (n,α_1) , and possibly at $\theta_L = 40^\circ$ for the (n,α_2) -

transition. This may suggest a participation of a compound process in the (n,α) reaction as there is also a known level in ^{10}Be observed by Tyren et al.¹⁰⁾ at (21.2 ± 2.6) MeV and by Garron et al.¹¹⁾ at (23.6 ± 1.5) MeV corresponding to an incident energy near 18 MeV.

Fig. 6 shows the energy dependence of the cross sections for the three transitions integrated over an angular range as large as possible. The angular distributions were integrated graphically. The error of the data points is estimated to be about 8 - 10 % due to the interpretation of the cross section shape and the graphical integration. A comparison of the integrated cross sections for the ground state transition with data available at the end of 1969⁹⁾, ¹²⁾, ¹³⁾ is shown in fig. 7. Because of the lack of data points at backward angles our integrated cross sections are generally lower than the data available. The shape of the excitation function integrated from 10° - 160° follow the slope of the data available at lower energies very well. The cross sections integrated over smaller angular ranges reflect the decreasing tendency of the known excitation function. For comparison some (p,α_0) data are given in the figure. The values at 15.6 and 18.6 MeV from Maxson¹³⁾ agree very well, also in the angular distributions not shown in this report. This good agreement gives evidence for independence of this reaction from the charge of the incoming particle as can be expected from the low Coulomb barrier height.

4. Conclusion

The measurement has shown that with this four parameter time-of-flight experiment two aims are achieved. First, different modes of joint reactions mechanisms can be determined - a detailed description of the analysis of the angular distributions is in progress. Second, data of neutron-induced reactions can simultaneously be measured and evaluated over a broad energy range up to about 30 MeV.

References

- 1) B. Duelli, G. Ries, Europ. Coll. on AVF Cycl., Eindhoven,
(April 1965)
S. Cierjacks, B. Duelli, P. Forti, D. Kopsch, L. Kropp, M. Lösel,
J. Nebe, H. Schweickert, and H. Unseld, Rev. Sci. Instr. 39,
1279, (1968)
- 2) G. Hartwig, W. Linder, M.E. Lösel, G. Schatz und H. Schweickert,
KFK 754 (1968)
- 3) L. Papadopoulos, Nucl. Instr. and Meth. 41, 241 (1966)
- 4) M.D. Goldberg, V.M. May, and R.S. Stehn, BNL 400 II. ed. Vol. 1
(1962)
A. Horsley, Nucl. Data A Vol. 2 (Acad. Press Inc. N.Y. and London,
1966)
- 5) F. Ajzenberg-Selove and T. Lauritsen, Nucl. Phys. 11, 1, (1959);
Nucl. Phys. 78, 1, (1966)
- 6) S.T. Butler, Phys. Rev. 106, 272, (1957)
G. Gambarini, I. Iori, S. Micheletti, N. Molho, M. Pignanelli,
and G. Tagliaferri, Nucl. Phys. A126, 562, (1969)
- 7) L. Kropp, thesis in preparation (1970)
L. Kropp, P. Forti, to be published
- 8) J. Hiura and T. Shimodaya, Progr. Theor. Phys. 30, 585, (1963)
- 9) G. Paic, D. Rendic, and P. Tomas, Nucl. Phys. A96, 476, (1967)

- 10) H. Tyren, S. Kulander, O. Sundberg, R. Ramachandran, and P. Isacsson, and T. Berggren, Nucl. Phys. 79, 321, (1966)
- 11) J.P. Garron, J.C. Jacmart, M. Riou, C. Ruhla, J. Teillac, and K. Strauch, Nucl. Phys. 37, 126, (1962)
- 12) M.E. Battat and F.L. Ribe, Phys. Rev. 89, 90, (1953)
P.H. Stelson and E.C. Campbell, Phys. Rev. 106, 1252, (1957)
S.S. Vasilev, V.V. Komarov, and A.M. Popova, JETP 6(33), 411, (1958)
K. Parker, AWRE Report O-27/60 (1960)
R. Bass, T.W. Bonner, and H.P. Haenni, Nucl. Phys. 23, 122, (1961)
S.A. Myachkova and V.P. Perelygin, JETP 13, 876, (1961)
S.T. Perkins, TID 22446 (1965)
H.R. Blieden, G.M. Temmer, and K.L. Warsh, Nucl. Phys. 49, 209, (1963)
- 13) D.R. Maxson, Phys. Rev. 128, 1321, (1962)
- 14) H.P. Yule, Nucl. Instr. and Meth. 54, 61, (1957)

Figure Caption

- Fig. 1 α -spectra from $\text{Be}^9(n,\alpha)$ for $E_n = (21.2 \pm 0.9)$ MeV and $\theta_{\text{Lab}} = 20, 40, 60, 80$ and 100°
- Fig. 2 Spectra of emitted α -particles for neutron energies between 8 and 30 MeV and $\theta_L = 20^\circ$ (a), 40° (b), 60° (c), 80° (d), and 100° (e)
- Fig. 3 Angular distributions of α -particles with energies corresponding to the three lowest states in He^6
- Fig. 4 Comparison of the angular distribution data at $E_n = 14.4$ MeV with data from Paic et al.⁹⁾
- Fig. 5 Excitation curves of the reaction $\text{Be}^9(n,\alpha)\text{He}^{6*}$ for various reaction angles and the transitions to the ground state (a) and the excited states at 1.7 MeV (b) and 3.4 MeV (c)
- Fig. 6 Integrated excitation functions for the reaction $\text{Be}^9(n,\alpha)\text{He}^{6*}$ (g. st., 1.7, 3.4 MeV)
- Fig. 7 Comparison with data available for the excitation function of $\text{Be}^9(n,\alpha)\text{He}^6$

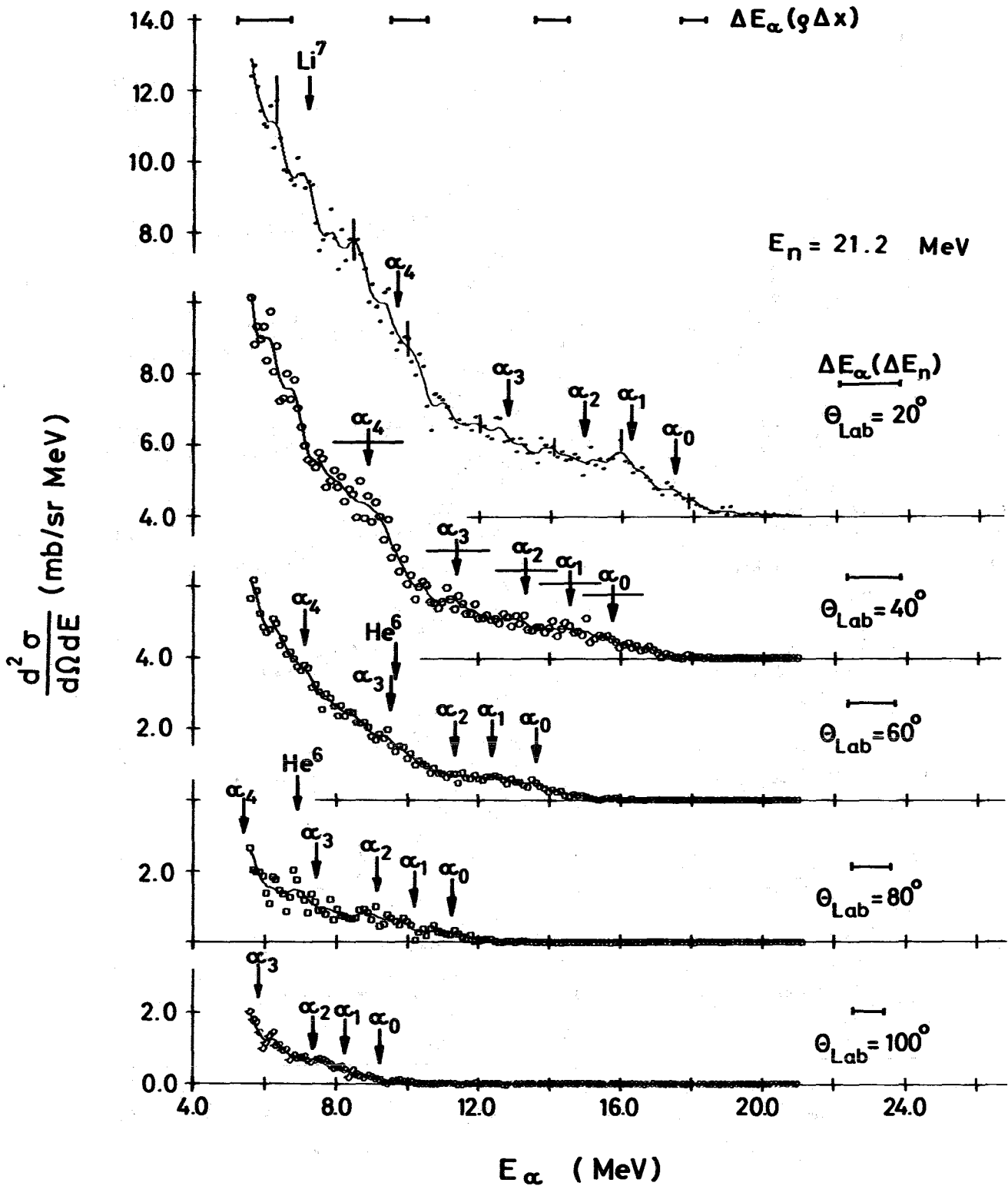


Fig. 1 $\text{Be}^9(n, \alpha)$ reaction cross section for $E_n = (21.2 \pm 0.9) \text{ MeV}$. The error bars above the reaction angles indicate the uncertainty in particle energy caused by time resolution, $\Delta E_\alpha (\Delta E_n)$. The solid lines represent the dependence after a 9-point smoothing¹⁴⁾.

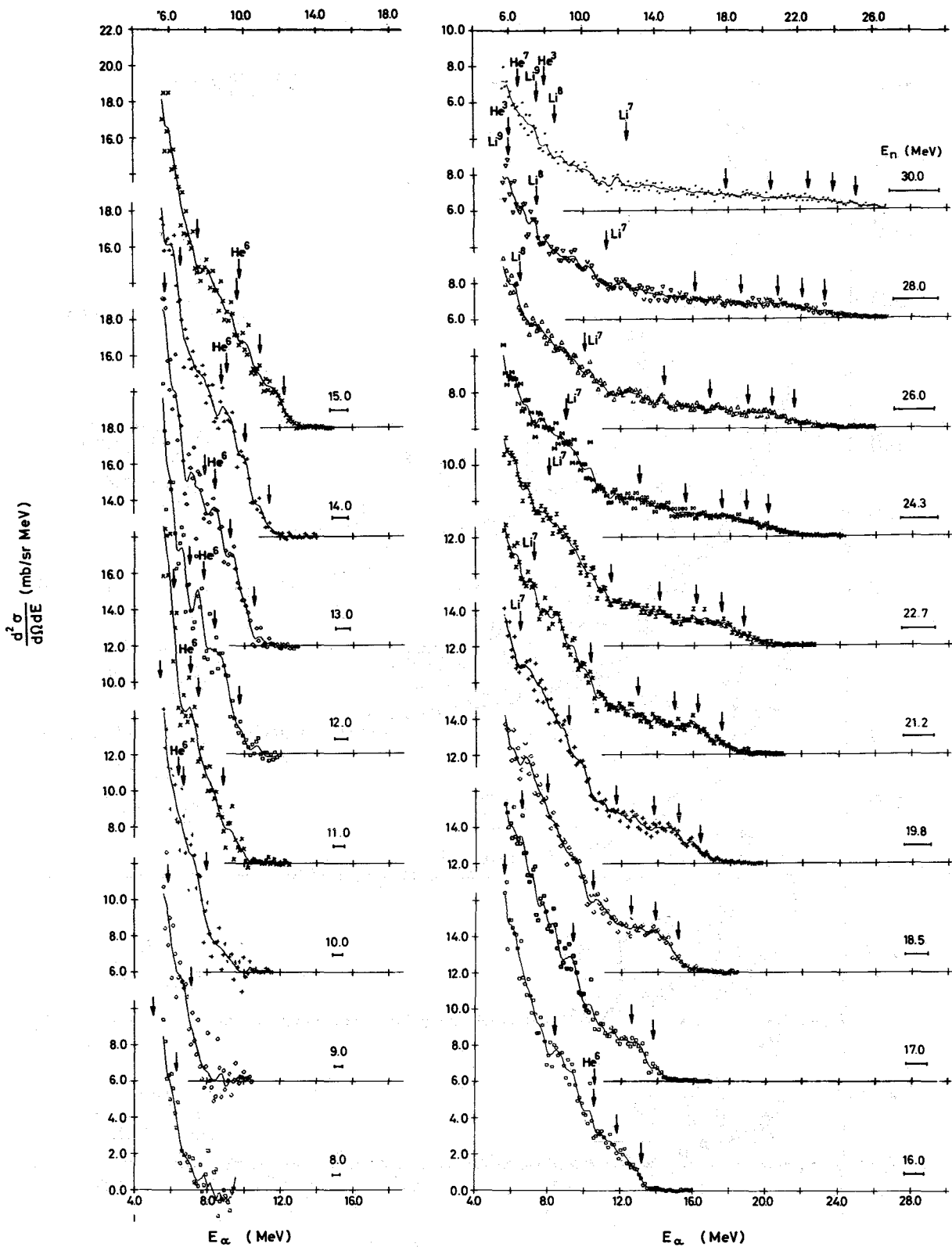


Fig. 2a Spectra of emitted α -particles from neutron interaction with Be^9 for $\theta_{\text{Lab}} = 20^\circ$.

The error bars under the parameter of neutron energy represent the uncertainty of α -particle energy due to time resolution

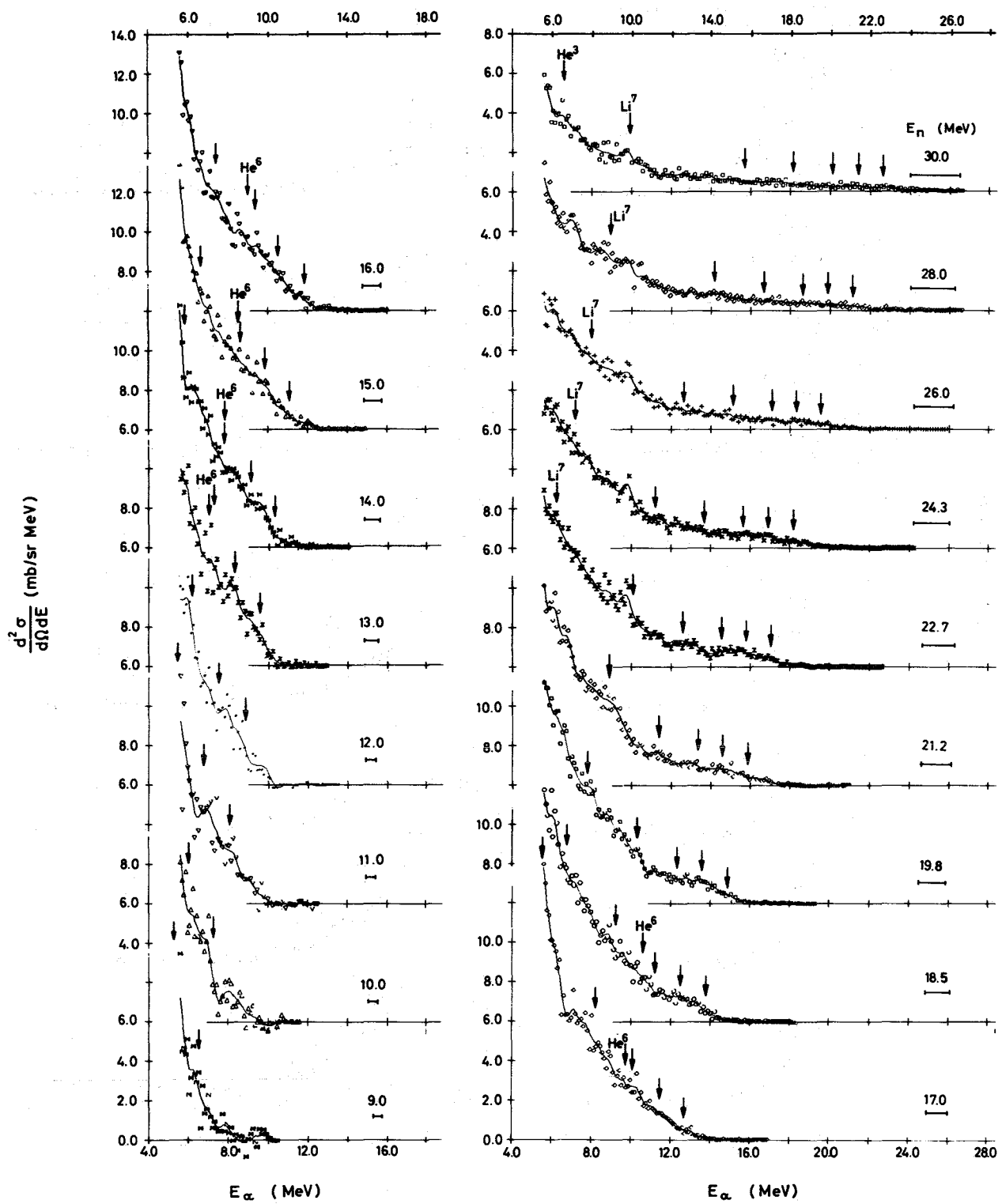


Fig. 2b Spectra of emitted α -particles for $\theta_{Lab} = 40^\circ$;
see also fig. 2a

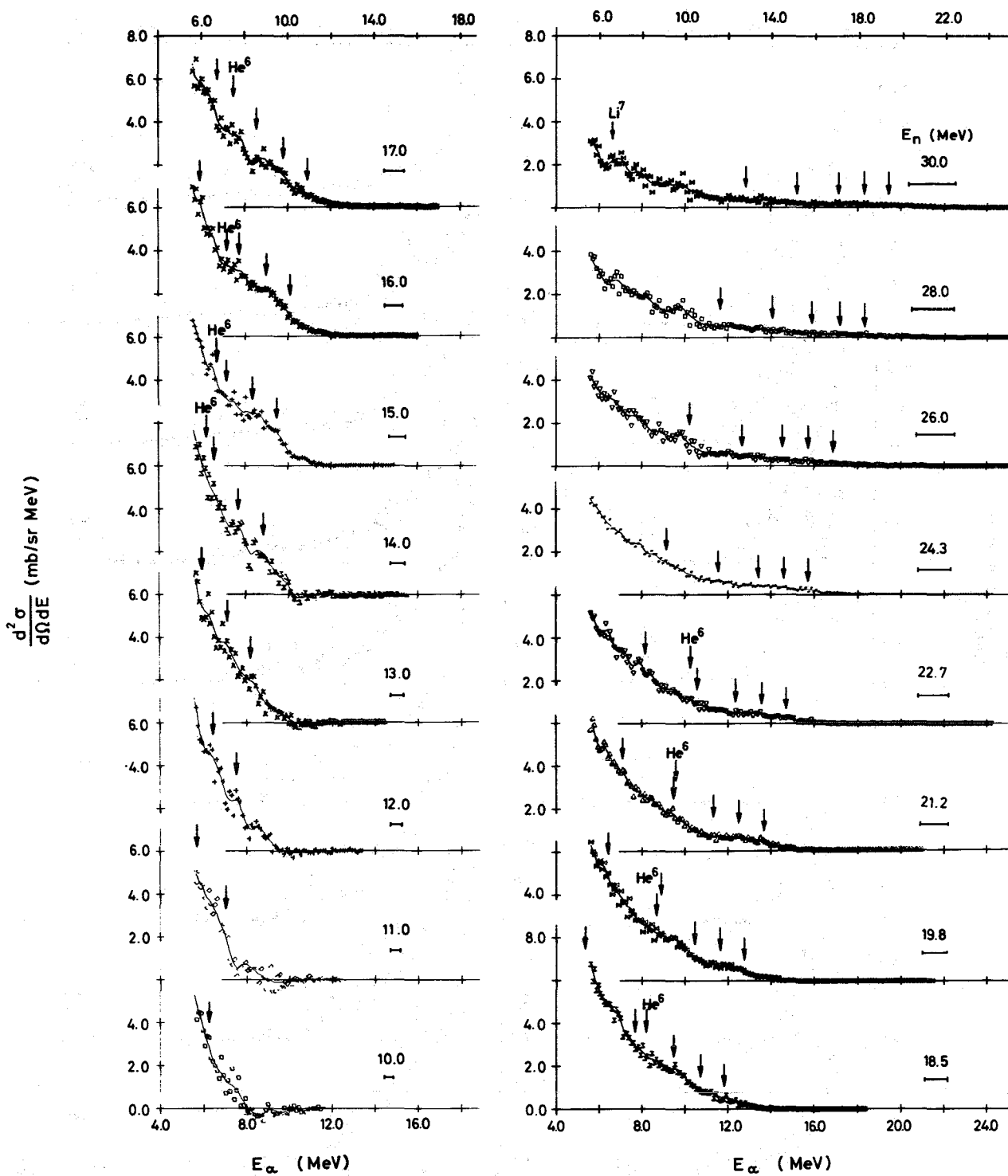


Fig. 2c Spectra of emitted α -particles for $\theta_{Lab} = 60^\circ$;
see also fig. 2a

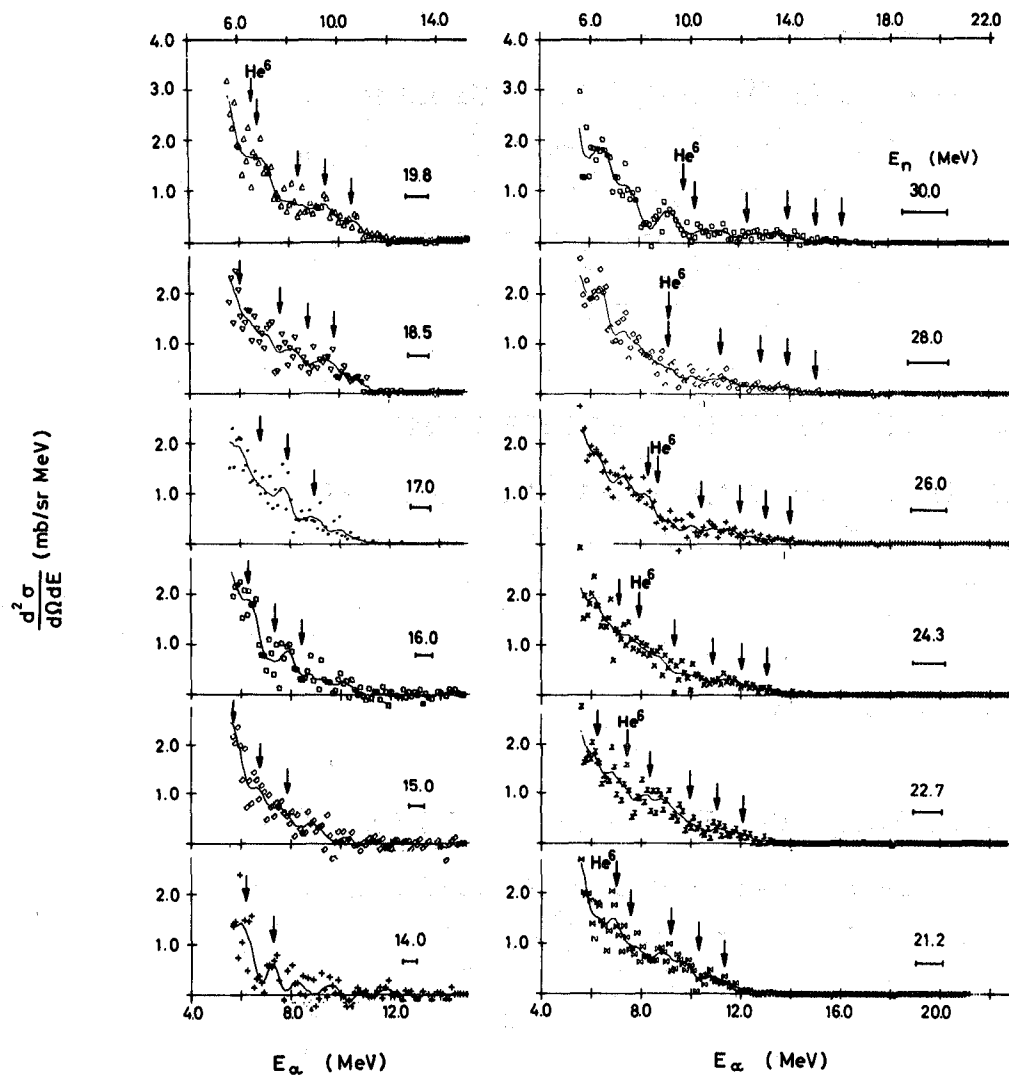


Fig. 2d Spectra of emitted α -particles for $\theta_{\text{Lab}} = 80^\circ$; see also fig. 2a

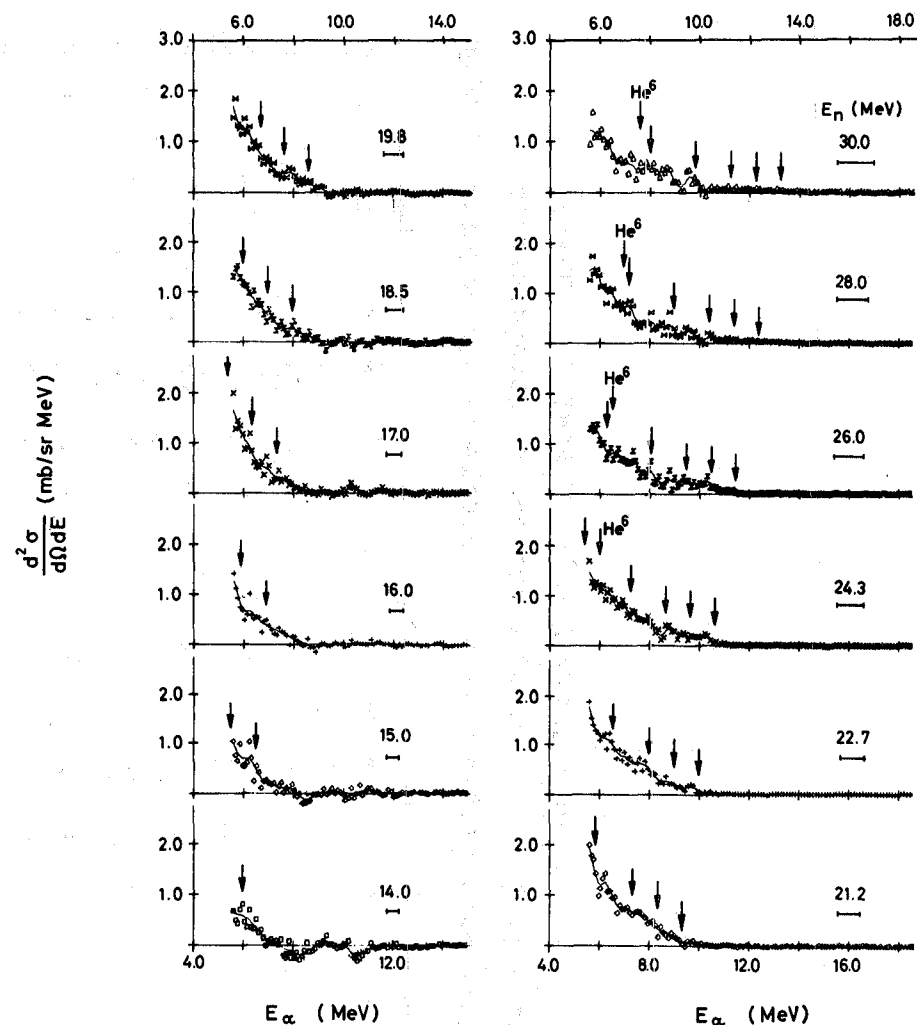


Fig. 2e Spectra of emitted α -particles for $\theta_{\text{Lab}} = 100^\circ$; see also fig. 2a

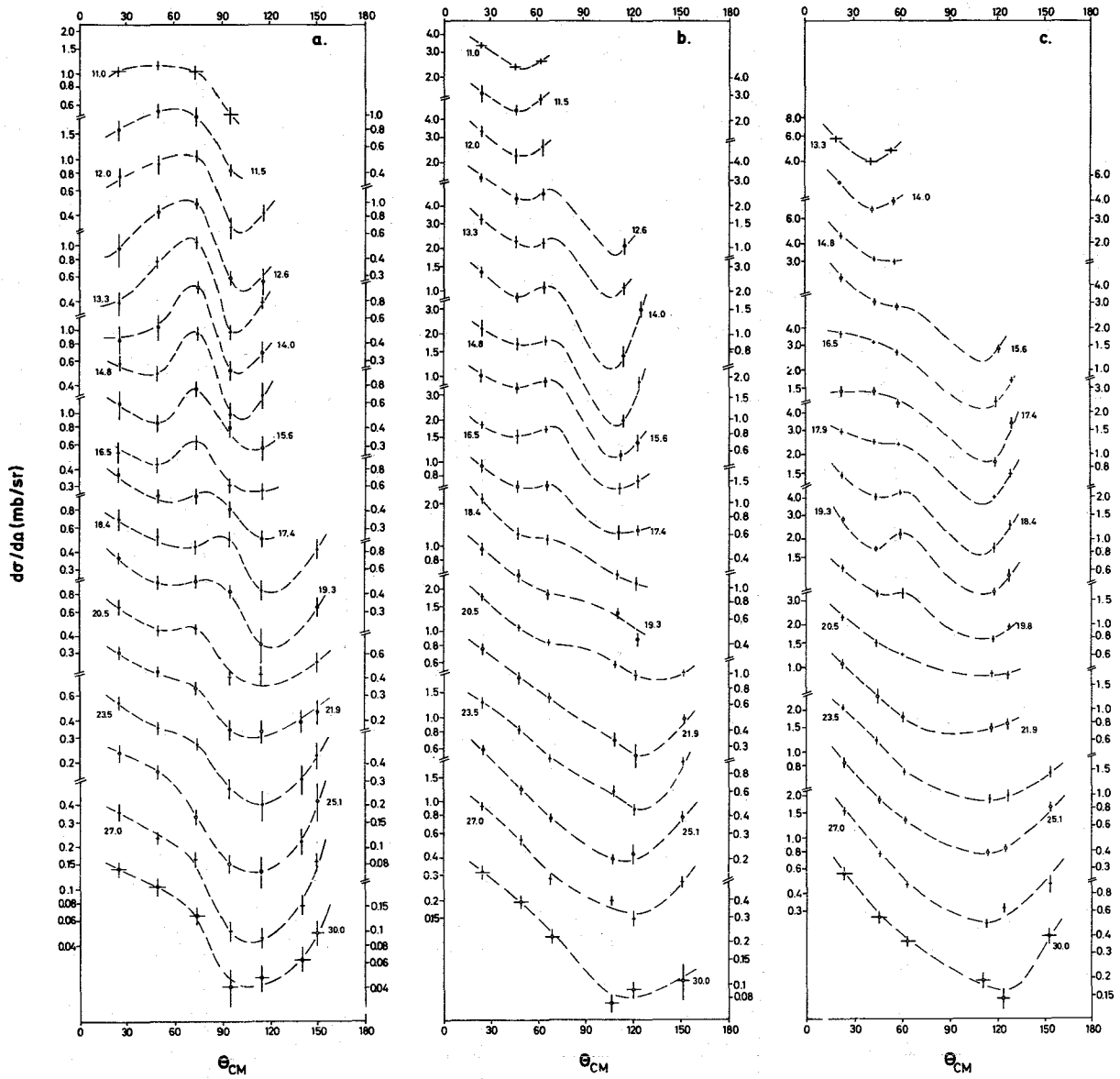


Fig. 3 Angular distributions of emitted α -particles with energies corresponding to the three lowest states in the He^6 -residual nucleus at 0, 1.7 and 3.4 MeV

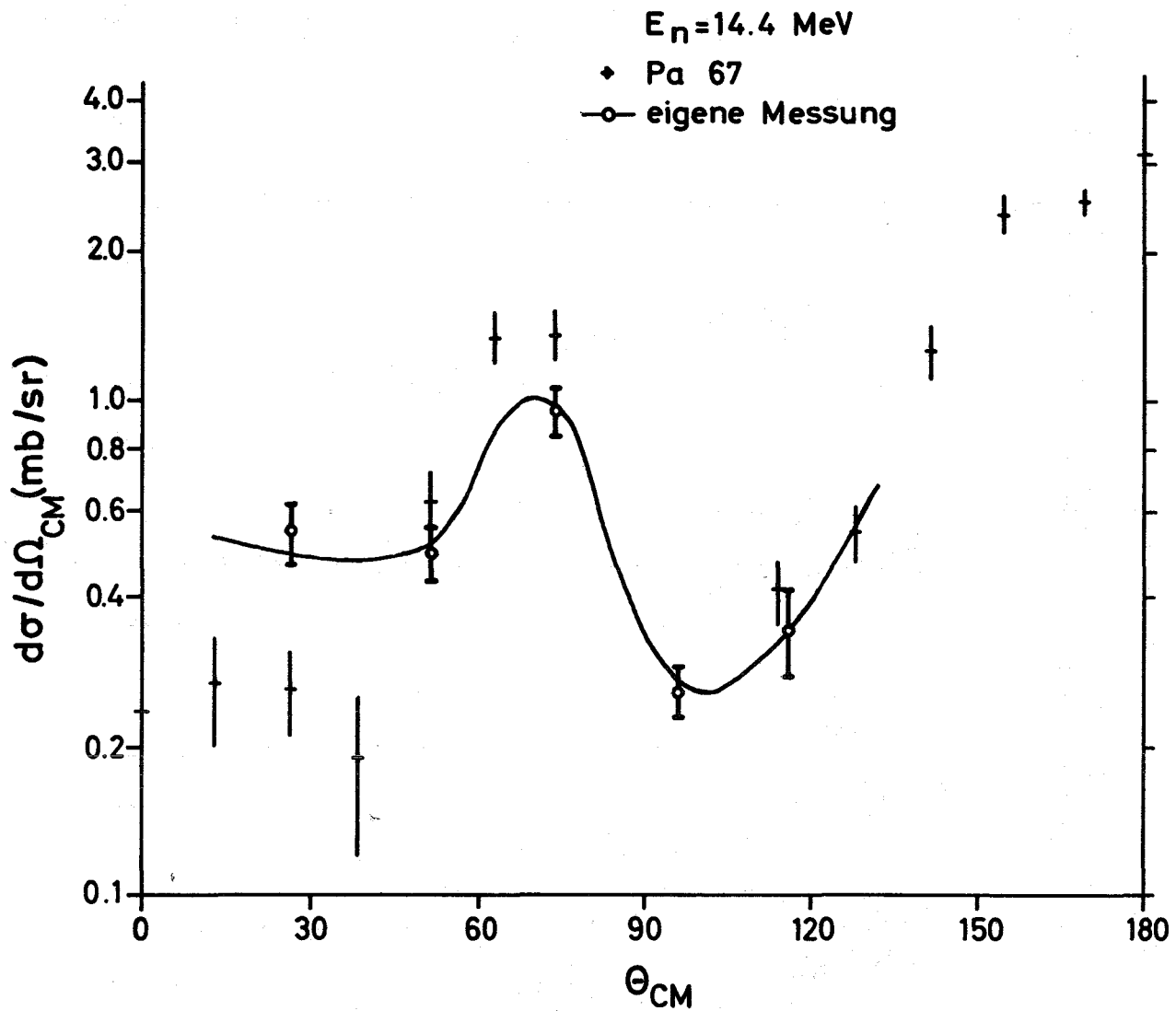


Fig. 4 Comparison of the 14.4 MeV angular distribution with the data from Paic et al. (ref. 9).

The solid line gives the continuous shape of the cross section over the $E_n - \Theta_{CM}$ plane as shown in fig. 3.

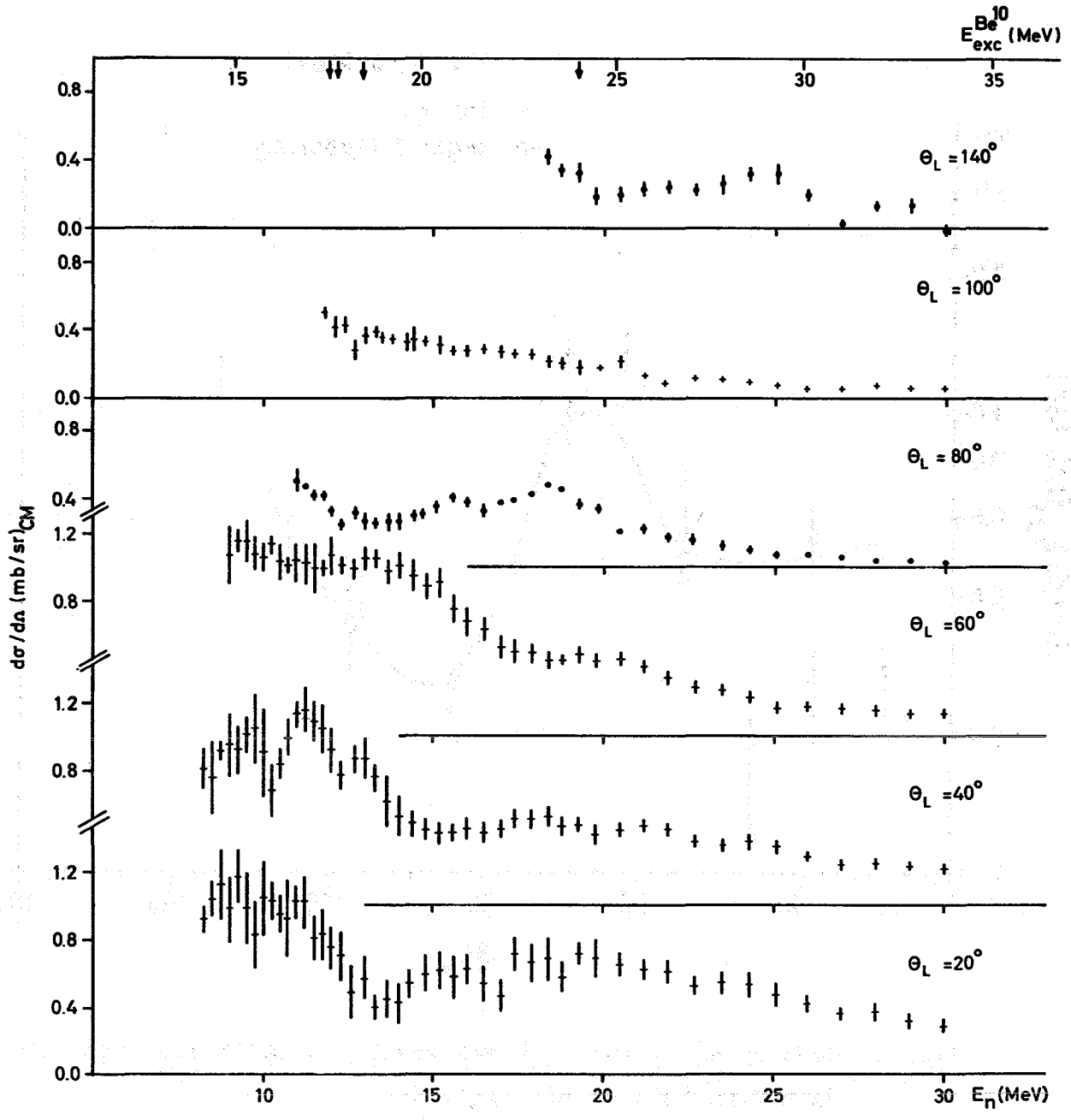


Fig. 5a Excitation curves for the reaction $Be^9(n, \alpha_0)He^6$ (g. st.) for various reaction angles

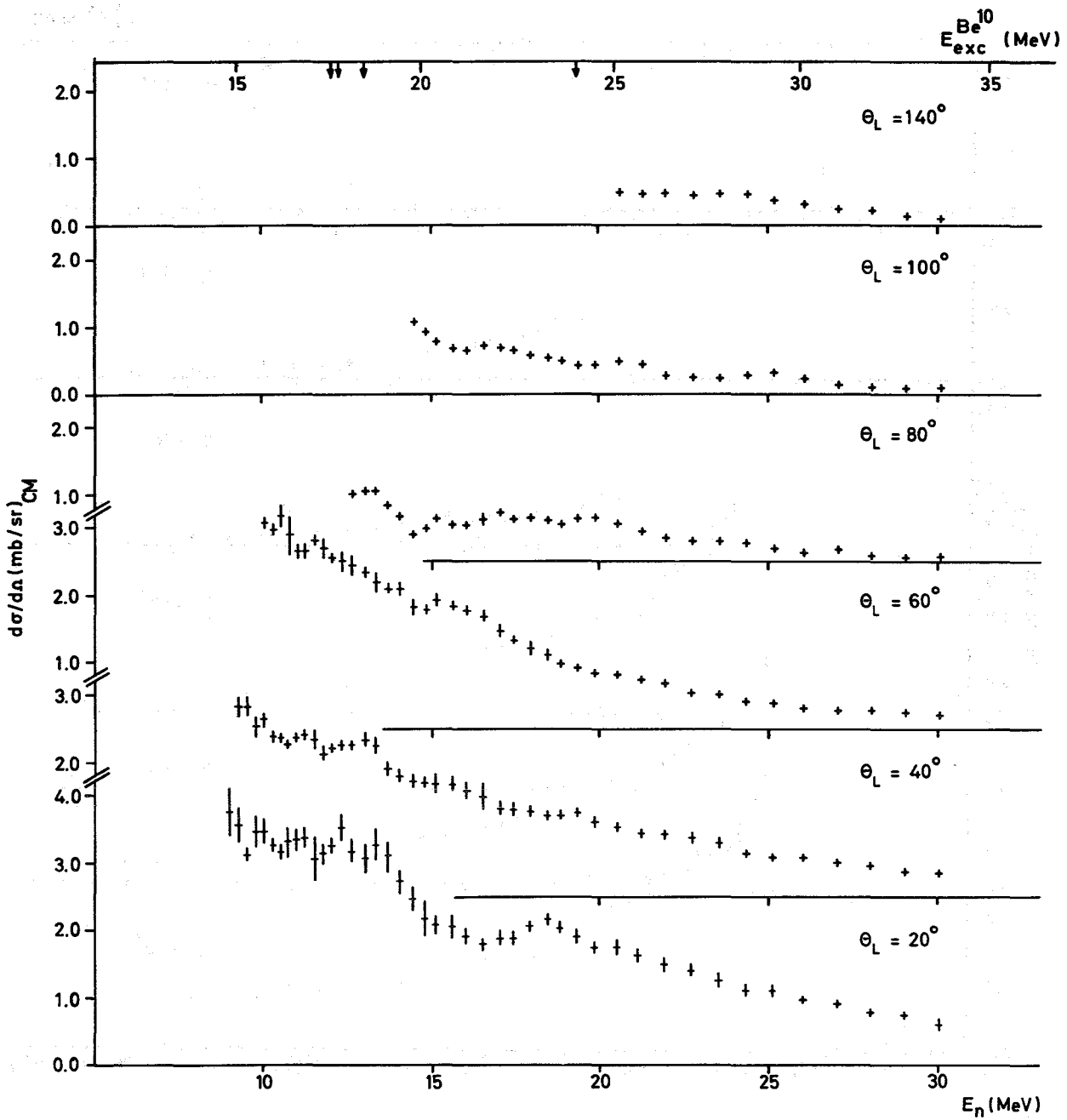


Fig. 5b Excitation curves for the reaction $Be^9(n, \alpha_1)He^6^*$ (1.7 MeV) for various reaction angles

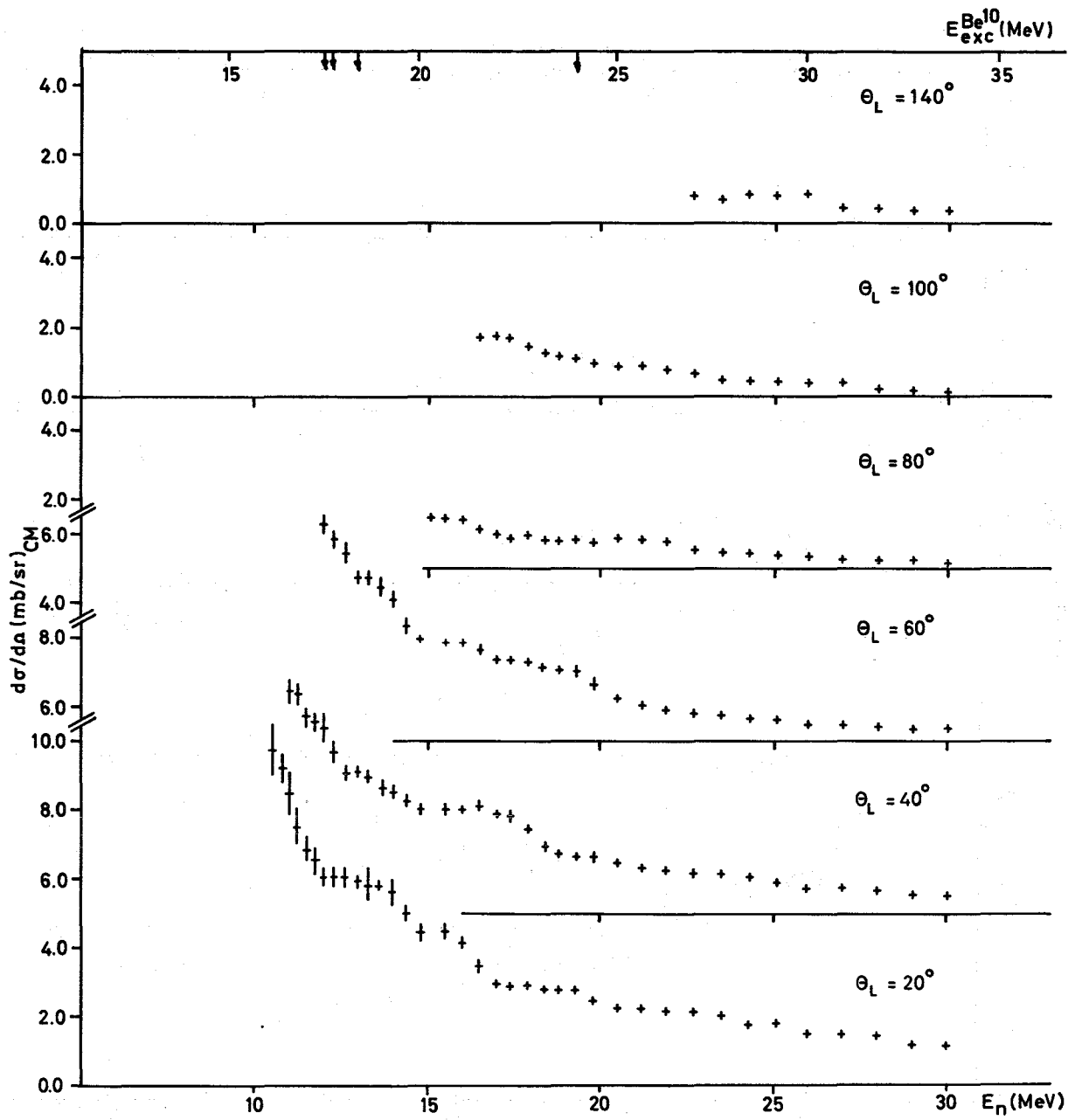


Fig. 5c Excitation curves for the reaction $Be^9(n, \alpha_2)He^{6*}$ (3.4 MeV) for various reaction angles

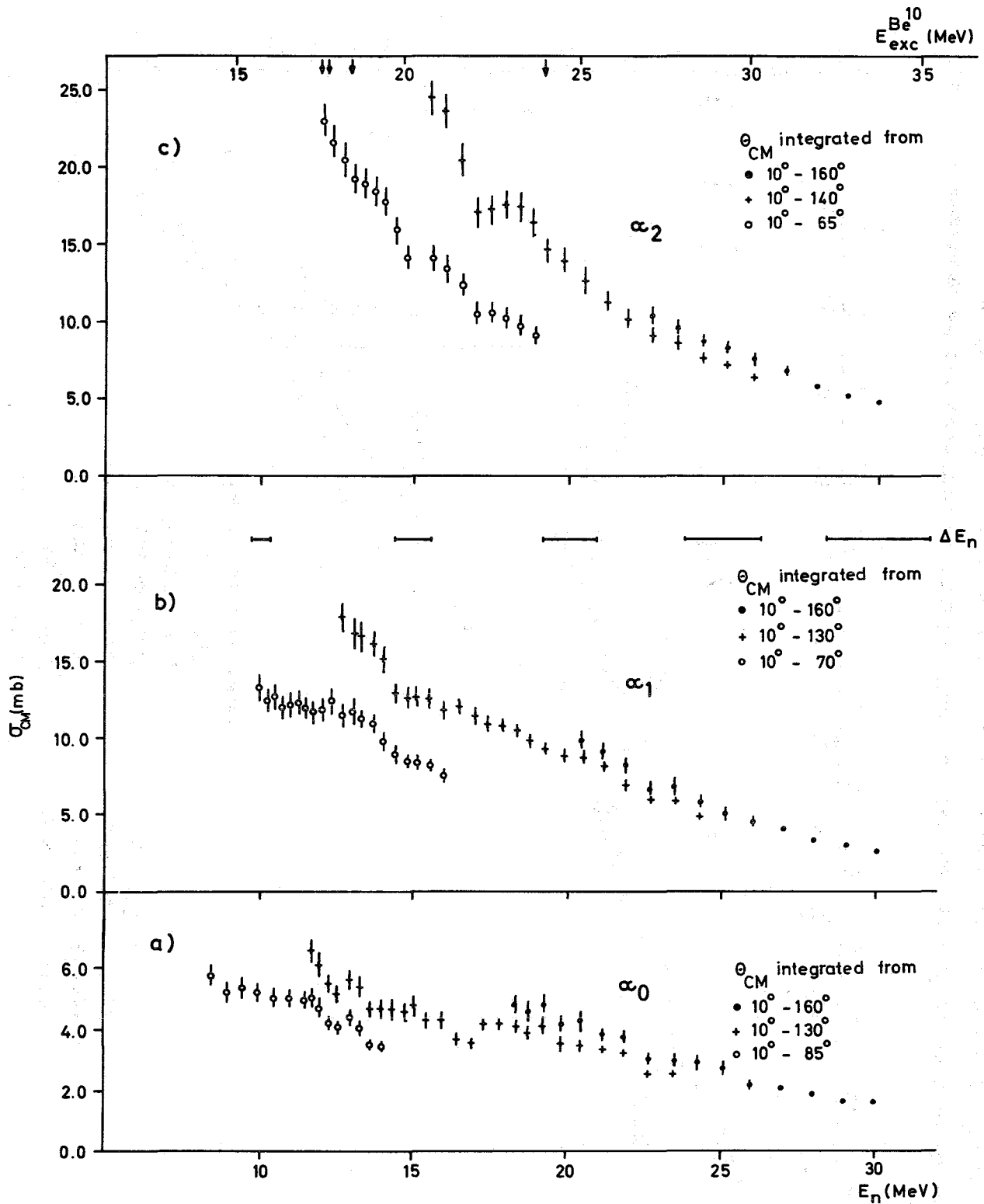


Fig. 6 Integrated excitation functions for a) $\text{Be}^9(n, \alpha_0)\text{He}^6(\text{g.s.t.})$, b) $\text{Be}^9(n, \alpha_1)\text{He}^6^*$ (1.7 MeV), c) $\text{Be}^9(n, \alpha_2)\text{He}^6^*$ (3.4 MeV). The range of angular integration is given in the figures. The uncertainty of neutron energy ΔE_n due to time resolution is indicated in part b) of the figure.

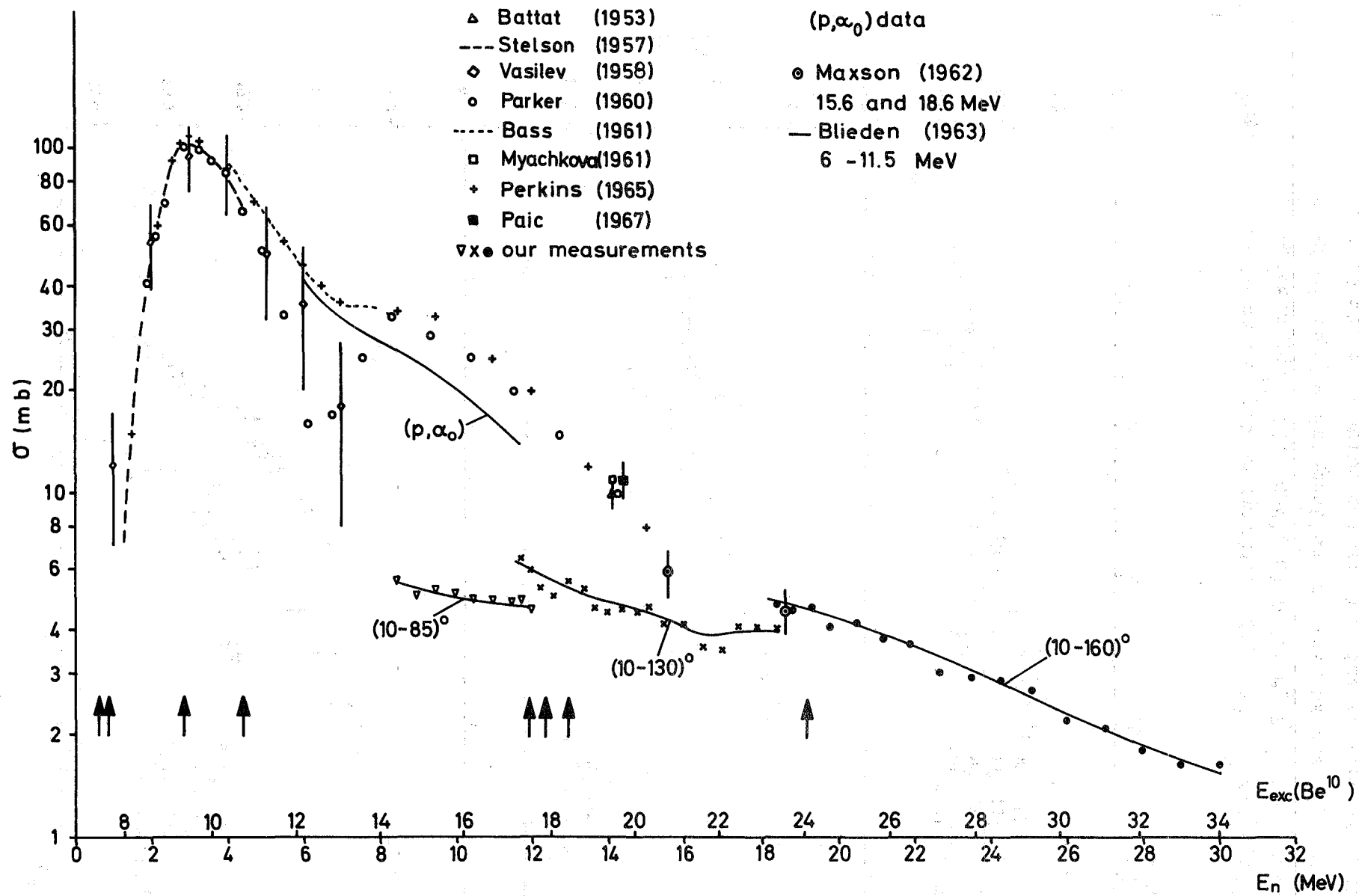


Fig. 7 Comparison of the measured excitation function for the ground state transition with data available by Dec. 1969. The arrows indicate known levels in the Be^{10} compound nucleus.